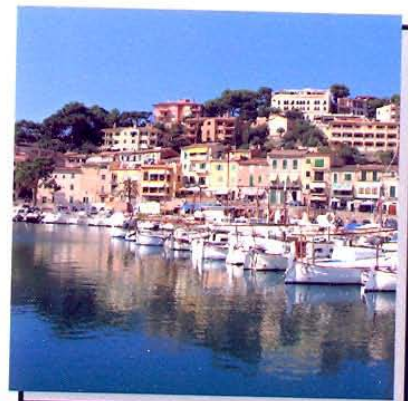
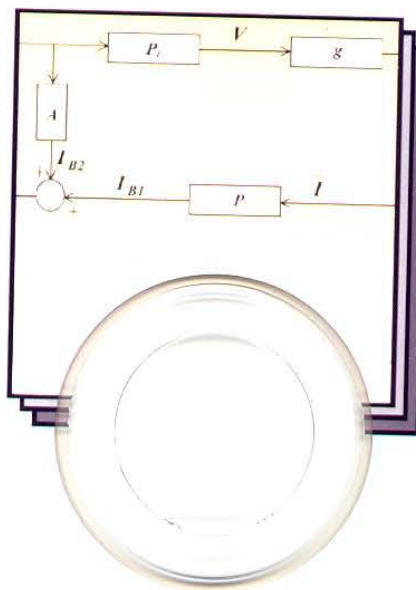
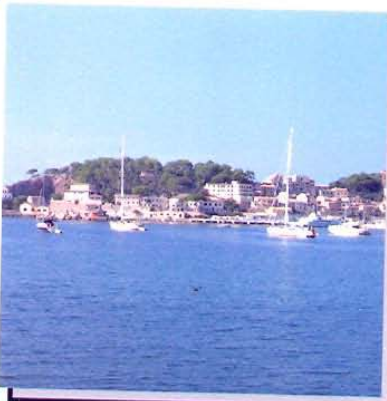




A Publication of the International Association
of Science and Technology for Development

581



Proceedings of the 16th IASTED International Conference on

Applied Simulation and Modelling

Editor: F. De Felice

August 29 – 31, 2007
Palma de Mallorca, Spain

ISBN: 978-0-88986-688-1

OPTIMAL ENERGY GAITS FOR QUADRUPEDS UNDER VARIABLE LOCOMOTION CONDITIONS

Manuel F. Silva and J. A. Tenreiro Machado
 Department of Electrical Engineering, Institute of Engineering of Porto,
 Rua Dr. António Bernardino de Almeida – 4200-072 Porto
 Portugal
 email: mss@isep.ipp.pt, jtm@isep.ipp.pt

ABSTRACT

This paper studies the adoption of periodic gaits of quadruped animals by multilegged artificial locomotion systems. The purpose is to determine the gait to adopt at different velocities, under distinct robot and locomotion conditions, based on two performance measures. A set of experiments reveals the influence of the gait and the body and ground parameters upon the proposed indices. It is verified that the gait should be adapted to the robot forward velocity and to the conditions under which the robot is moving. The experiments also reveal that a gait that decreases the energy consumption generally implies an increase in the trajectory following errors.

KEY WORDS

Robotics, locomotion, gait, modelling, simulation

1. Introduction

Due to their intrinsic characteristics, walking machines allow locomotion in terrain inaccessible to other type of vehicles. For this to become fully possible, gait analysis is a research area requiring an appreciable modelling effort for the improvement of mobility with legs in unstructured environments. Several robots have been developed which adopt different gaits such as the bound [1, 2], trot [3] and gallop [4]. Nevertheless, detailed studies on the best set of gait and locomotion variables for different robot velocities are scarce [5, 11].

In this line of thought, a simulation model for multilegged locomotion systems was developed for several periodic gaits [6]. Based on this model, we test the quadruped robot locomotion, as a function of the forward velocity V_F , when adopting different periodic gaits often observed in several quadruped animals while they walk and run [7].

This study intends to generalize previous work [8, 9] through the study of the cost of robot movement during forward straight line displacement at different velocities. First, a set of simulation experiments are developed to estimate the optimum values for the parameters step length L_S and body height H_B , during the robot locomotion, while the robot is moving along the planned

trajectories. Next, is determined the best locomotion gait in the velocity range $0.1 \leq V_F \leq 10.0 \text{ ms}^{-1}$, from the viewpoint of energy efficiency, being the controller tuned for each particular locomotion velocity, while minimizing the proposed index E_{av} , and adopting the optimum locomotion parameters L_S and H_B . These experiments are repeated for distinct characteristics of the robot body and of the ground.

Bearing these facts in mind, the paper is organized as follows. Section two introduces the robot model. Sections three and four present the robot motion planning and control architecture and the optimizing indices, respectively. Section five develops a set of experiments that reveal the influence of the locomotion parameters and robot gaits upon the performance measures, as a function of robot body velocity. Finally, section six outlines the main conclusions.

2. Robot Kinematic and Dynamic Models

2.1 Robot Kinematic Model

We consider a quadruped walking system (Figure 1) with $n = 4$ legs, equally distributed along both sides of the robot body, having each two rotational joints (*i.e.*, $j = \{1, 2\} \equiv \{\text{hip, knee}\}$).

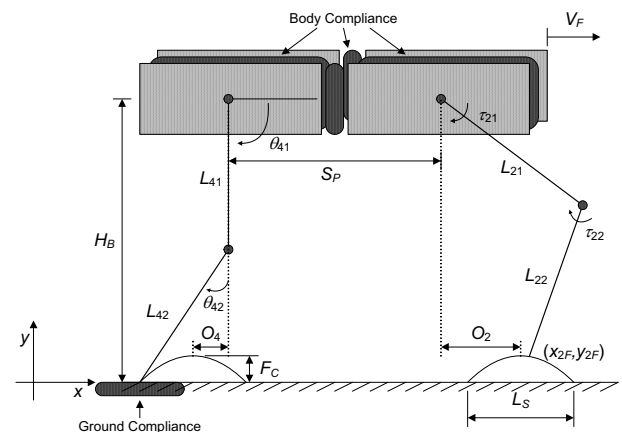


Fig. 1. Kinematic and dynamic quadruped robot model.

TABLE I
SYSTEM PARAMETERS

Robot model parameters		Locomotion parameters	
S_P	1 m	L_S	1 m
L_{ij}	0.5 m	H_B	0.9 m
O_i	0 m	F_C	0.1 m
M_b	88.0 kg		
M_{ij}	1 kg	Ground parameters	
K_{xH}	10^5 Nm^{-1}	K_{xF}	$1.3 \times 10^6 \text{ Nm}^{-1}$
K_{yH}	10^4 Nm^{-1}	K_{yF}	$1.7 \times 10^6 \text{ Nm}^{-1}$
B_{xH}	10^3 Nsm^{-1}	B_{xF}	$2.3 \times 10^6 \text{ Nsm}^{-1}$
B_{yH}	10^2 Nsm^{-1}	B_{yF}	$2.7 \times 10^6 \text{ Nsm}^{-1}$

The kinematic model comprises a set of parameters that allow the complete description of the robot movement, namely, the cycle time T , the duty factor β , the transference time $t_T = (1-\beta)T$, the support time $t_S = \beta T$, the step length L_S , the stroke pitch S_P , the body height H_B , the maximum foot clearance F_C , the i^{th} leg lengths L_{i1} and L_{i2} and the foot trajectory offset O_i ($i = 1, \dots, n$).

2.2 Inverse Dynamics Computation

The model for the robot inverse dynamics is formulated as:

$$\Gamma = \mathbf{H}(\Theta)\ddot{\Theta} + \mathbf{c}(\Theta, \dot{\Theta}) + \mathbf{g}(\Theta) - \mathbf{F}_{RH} - \mathbf{J}_F^T(\Theta)\mathbf{F}_{RF} \quad (1)$$

where Γ is the vector of forces / torques, Θ is the vector of position coordinates, $\mathbf{H}(\Theta)$ is the inertia matrix and $\mathbf{c}(\Theta, \dot{\Theta})$ and $\mathbf{g}(\Theta)$ are the vectors of centrifugal / Coriolis and gravitational forces / torques, respectively [6]. The matrix $\mathbf{J}_F^T(\Theta)$ is the transpose of the robot Jacobian matrix, \mathbf{F}_{RH} is the vector of the body inter-segment forces and \mathbf{F}_{RF} is the vector of the reaction forces that the ground exerts on the robot feet. These forces are null during the foot transfer phase. During the system simulation, Eq. (1) is integrated through the Runge-Kutta method. Furthermore, we consider that the joint actuators are not ideal, exhibiting saturation, being τ_{ijMax} the maximum torque that the actuator can supply.

2.3 Robot Dynamic Model

Regarding the robot dynamic model (Figure 1), it is considered robot body compliance because most walking animals have a spine that allows supporting the locomotion with improved stability.

The robot body is divided in n identical segments (each with mass M_i) and a linear spring-damper system is adopted to implement the intra-body compliance [6]. The parameters of this model ($K_{\eta H}$ and $B_{\eta H}$) are defined so that the body behaviour is similar to the one expected to occur on an animal (Table I) [6].

The contact of the robot feet with the ground is modelled through a non-linear system [6], with linear stiffness $K_{\eta F}$ and non-linear damping $B_{\eta F}$, being the values for the model parameters $K_{\eta F}$ and $B_{\eta F}$ (Table I) based on the

studies of soil mechanics, assuming that the ground is of compact clay [6].

3. Robot Trajectory Planning and Control

3.1 Hips, Feet and Joints Trajectory Planning

Gaits describe sequences of leg movements, alternating between transfer and support phases. Given a particular gait and duty factor β , it is possible to calculate, for leg i , the corresponding phase ϕ_i , the time instant where each leg leaves and returns to contact with the ground and the cartesian trajectories of the tip of the feet (that must be completed during t_T) [6].

We consider a periodic trajectory for each foot, with body velocity $V_F = L_S / T$. Based on this data, the trajectory generator is responsible for producing a motion that synchronizes and coordinates the legs.

The robot body, and by consequence the legs hips, is assumed to have a desired horizontal movement with a constant forward speed V_F . Therefore, for leg i the cartesian coordinates of the hip of the legs are given by $\mathbf{p}_{Hd}(t) = [x_{iHd}(t), y_{iHd}(t)]^T$:

$$\mathbf{p}_{Hd}(t) = [V_F t + S_P(1 - \text{ceil}(i/2)) \quad H_B]^T \quad (2)$$

Regarding the feet trajectories, for each cycle the desired geometric trajectory of the foot of the swing leg is computed through a cycloid function (Eq. 3a) [6]. For example, considering that the transfer phase starts at $t = 0$ s for leg $i = 1$ we have for $\mathbf{p}_{Fd}(t) = [x_{iFd}(t), y_{iFd}(t)]^T$:

- during the transfer phase:

$$\mathbf{p}_{Fd}(t) = \left[V_F \left[t - \frac{t_T}{2\pi} \sin\left(\frac{2\pi t}{t_T}\right) \right], \frac{F_C}{2} \left[1 - \cos\left(\frac{2\pi t}{t_T}\right) \right] \right]^T \quad (3a)$$

- during the stance phase:

$$\mathbf{p}_{Fd}(t) = [V_F T \quad 0]^T \quad (3b)$$

The algorithm for the forward motion planning accepts the desired cartesian trajectories of the leg hips $\mathbf{p}_{Hd}(t)$ and feet $\mathbf{p}_{Fd}(t)$ as inputs and, by means of an inverse kinematics algorithm Ψ^{-1} , generates the related joint trajectories $\Theta_d(t) = [\theta_{1d}(t), \theta_{2d}(t)]^T$, selecting the solution corresponding to a forward knee [6].

3.2 Control Architecture

The general control architecture of the quadruped robot is presented in Figure 2. The planned joint trajectories $\Theta_d(t)$ constitute the reference for the robot control system. Since the trajectory planning is carried out in the cartesian space but the control is performed in the joint space, it is required the integration of the inverse kinematic model in the forward path. The control algorithm includes an external position feedback loop and an internal loop with information of the foot-ground interaction force.

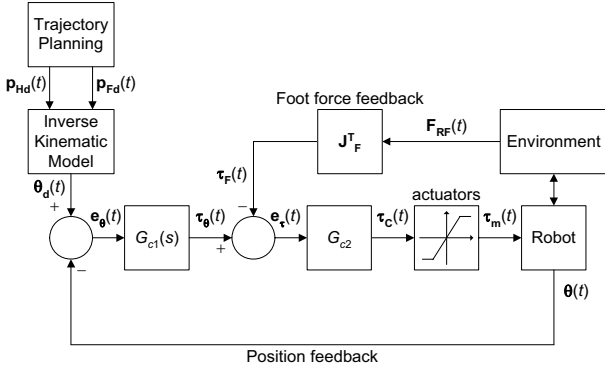


Fig. 2. Quadruped robot control architecture.

For $G_{c1}(s)$ we adopt a PD controller and for G_{c2} a simple P controller [10].

4. Metrics for Performance Evaluation

We establish two global measures of the overall performance of the mechanism in an average sense. One index is inspired on the system dynamics $\{E_{av}\}$ and the other is based on the trajectory tracking errors $\{\mathcal{E}_{xyH}\}$ [11]. The performance optimization requires the minimization of each index.

The first index, the mean absolute density of energy per travelled distance E_{av} , is computed assuming that energy regeneration is not available by actuators doing negative work (by taking the absolute value of the power). At a given joint j (each leg has $m = 2$ joints) and leg i (since we are adopting a quadruped it yields $n = 4$ legs), the mechanical power is the product of the motor torque and angular velocity. The global index E_{av} is obtained by averaging the mechanical absolute energy delivered over the travelled distance d :

$$E_{av} = \frac{1}{d} \sum_{i=1}^n \sum_{j=1}^m \int_0^T |\tau_{ij}(t) \dot{\theta}_{ij}(t)| dt \quad [\text{Jm}^{-1}] \quad (4)$$

In what concerns the hip trajectory following errors we define the index:

$$\mathcal{E}_{xyH} = \sum_{i=1}^n \sqrt{\frac{1}{N_s} \sum_{k=1}^{N_s} (\Delta_{ixH}^2 + \Delta_{iyH}^2)} \quad [\text{m}] \quad (5)$$

$$\Delta_{ixH} = x_{iHd}(k) - x_{iH}(k), \Delta_{iyH} = y_{iHd}(k) - y_{iH}(k)$$

where N_s is the total number of samples for averaging purposes and $\{d, r\}$ indicate the i^{th} samples of the desired and real position, respectively.

5. Simulation Results

To illustrate the use of the preceding concepts, in this section we develop a set of simulation experiments to estimate the influence of the robot body and ground parameters, on the quadruped energy consumption and trajectory following errors, when adopting periodic gaits.

TABLE II
QUADRUPED GAIT PARAMETERS

Gait	ϕ_1	ϕ_2	ϕ_3	ϕ_4	β
Walk	0	0.5	0.75	0.25	0.65
Chelonian Walk	0	0.5	0.5	0	0.8
Amble	0	0.5	0.75	0.25	0.45
Trot	0	0.5	0.5	0	0.4
Pace	0	0.5	0	0.5	0.4
Canter	0	0.3	0.7	0	0.4
Transverse Gallop	0	0.2	0.6	0.8	0.3
Rotary Gallop	0	0.1	0.6	0.5	0.3
Half-Bound	0.7	0.6	0	0	0.2
Bound	0	0	0.5	0.5	0.2

We consider three walking gaits (Walk, Chelonian Walk and Amble), two symmetrical running gaits (Trot and Pace) and five asymmetrical running gaits (Canter, Transverse Gallop, Rotary Gallop, Half-Bound and Bound). These are the gaits usually adopted by animals moving at low, moderate and high speed, respectively, being their main characteristics presented in Table II.

In a first phase, the experiments consist in estimating the optimum values for the parameters step length L_S and body height H_B versus V_F , during the robot locomotion with a periodic gait and while the robot is moving along the planned trajectories.

In a second phase we determine the best locomotion gait, from the viewpoint of energy efficiency, in the velocity range $0.1 \leq V_F \leq 10.0 \text{ ms}^{-1}$. The controller is tuned for each particular locomotion velocity, while minimizing the index E_{av} , and adopting the (optimum) locomotion parameters L_S and H_B determined in the previous phase. These experiments are repeated for distinct values of the robot intra-body compliance parameters, since animals use their body compliance to store energy at high velocities, and for different characteristics of ground, since walking robots are intended to move on different types of terrains.

For the system simulation we consider the robot body parameters, the locomotion parameters and the ground parameters presented in Table I. Moreover, we assume high performance joint actuators with a maximum torque of $\tau_{ijMax} = 400 \text{ Nm}$. To tune the controller we adopt a systematic method, testing and evaluating a grid of several possible combinations of controller parameters, while minimising E_{av} .

5.1 Locomotion Parameters versus V_F

To analyse the evolution of the locomotion parameters L_S and H_B with V_F we test the forward straight line planned quadruped robot locomotion, as a function of V_F , when adopting different gaits often observed in several quadruped animals while they walk/run at variable speeds (Table II) [7].

With this purpose, the robot planned forward straight line locomotion is simulated for the different gaits, while varying the body velocity on the range $0.2 \leq V_F \leq 10.0 \text{ ms}^{-1}$. For each gait and body velocity, is

determined the set of locomotion parameters (L_S , H_B) that minimises the performance index E_{av} .

We conclude that the minimum values of the index E_{av} increase with V_F , independently of the adopted locomotion gait. Furthermore, gaits with higher values of β show a higher increase of E_{av} [9].

It is also important to analyse how the locomotion parameters vary with V_F . Figure 3 shows, for three locomotion gaits, that the optimal value of L_S must increase with V_F when considering E_{av} . Figure 4 shows that H_B must decrease with V_F from the viewpoint of the same performance index.

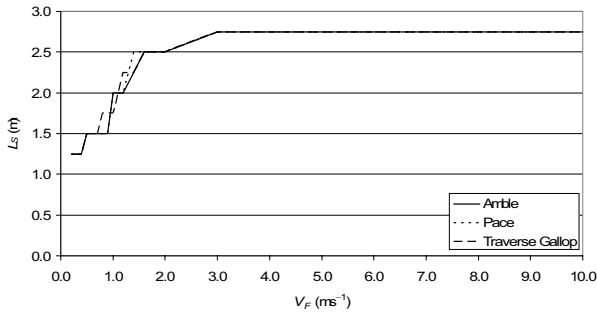


Fig. 3. $L_S(V_F)$ for $\min(E_{av})$, with $F_C = 0.1$ m.

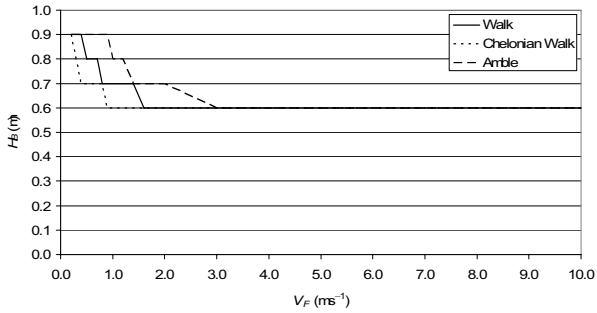


Fig. 4. $H_B(V_F)$ for $\min(E_{av})$, with $F_C = 0.1$ m.

For the other periodic walking gaits considered on this study, the evolution of E_{av} and (L_S , H_B) with V_F follows the same pattern. Therefore, we conclude that the locomotion parameters should be adapted to the walking velocity in order to optimize the robot performance. As V_F increases, the value of H_B should decrease and the value of L_S should increase. These results seem to agree with the observations of the living quadruped creatures [12].

5.2 Gait Selection versus V_F when Varying L_S and H_B

To analyse the influence of L_S and H_B in the locomotion performance, in the sequel we determine the best locomotion gait, from the viewpoint of the minimization of E_{av} , at each forward velocity in the range $0.1 \leq V_F \leq 10.0$ ms^{-1} . The controller is tuned for each particular case, while minimizing E_{av} , and adopting for each gait and value of V_F , the parameters L_S and H_B determined in sub-section 5.1.

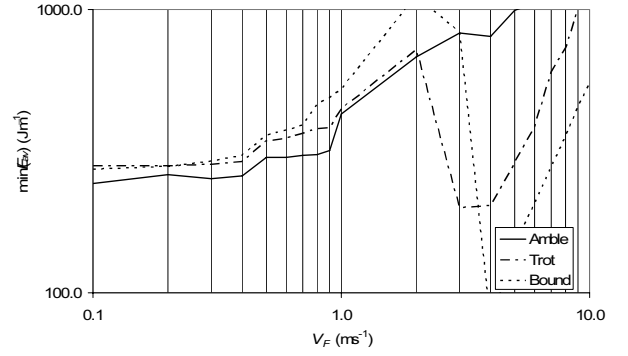


Fig. 5. $\min[E_{av}(V_F)]$ for $F_C = 0.1$ m, considering the optimum values of L_S and H_B and the base parameters for the robot intra-body compliance and ground characteristics.

Figure 5 presents the chart of $\min[E_{av}(V_F)]$. This index points out that the locomotion should switch from Amble, to Trot and to Bound, as the speed increases. The other gaits under consideration present higher values of $\min[E_{av}(V_F)]$, on all range of V_F under consideration. In particular, the gaits Walk and Chelonian Walk reveal the higher values of this performance measure.

5.3 Gait Selection versus V_F for a Stiff Body

The experiments performed in the previous section are now repeated for the case of assuming a stiff robot body. For this case, and considering the base parameters presented in Table I, the values of the robot body intra-compliance defining parameters $\{K_{xH}$, B_{xH} , K_{yH} and $B_{yH}\}$ are varied simultaneously through a factor $K_{mult} = 10$. For this case, the chart of $\min[E_{av}(V_F)]$, for the different gaits, is presented in Figure 6.

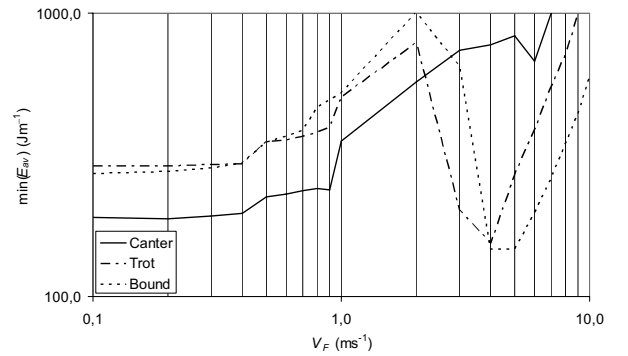


Fig. 6. $\min[E_{av}(V_F)]$ for $F_C = 0.1$ m, considering the optimum values of L_S and H_B and a robot with a stiff body.

From the analysis of this figure, it is concluded that the most efficient way of performing the locomotion, measured through the index E_{av} , is to adopt the Canter gait for $V_F < 2.0$ ms^{-1} , the Trot gait for 2.0 $\text{ms}^{-1} < V_F < 4.0$ ms^{-1} and the Bound gait for $V_F > 4.0$ ms^{-1} . All the remaining gaits under study present values of

$\min[E_{av}(V_F)]$ higher than these ones, for all range of V_F under consideration.

Such as in the previous case, we observe that for values of $V_F > 2 \text{ ms}^{-1}$ there is a strong decreasing in the values of $\min[E_{av}(V_F)]$ for the Trot and Bound gaits.

5.4 Gait Selection versus V_F for a Soft Body

The study that is being developed is now repeated for the case of assuming a soft robot body. Therefore, considering the base parameters presented in Table I, the values of the robot body intra-compliance defining parameters $\{K_{xH}, B_{xH}, K_{yH}$ and $B_{yH}\}$ are varied simultaneously through a factor $K_{mult} = 0.1$.

Figure 7 presents the chart of $\min[E_{av}(V_F)]$ for the different gaits. The index E_{av} suggests that the locomotion should be Trot, Pace, Bound and Half-Bound, as the speed increases. The other gaits under consideration present values of $\min[E_{av}(V_F)]$ higher than these ones, for all range of V_F .

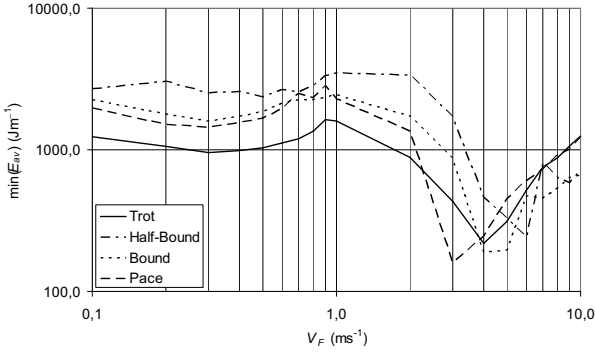


Fig. 7. $\min[E_{av}(V_F)]$ for $F_C = 0.1 \text{ m}$, considering the optimum values of L_S and H_B , and a robot with a soft body.

Comparing the results for this situation, with those of the previous cases, it is observed that for $V_F < 2.0 \text{ ms}^{-1}$ a soft body demands higher values of $\min[E_{av}(V_F)]$. Moreover, the hip trajectory following errors, measured through ε_{xyH} , are also higher for all values of V_F in the range under study.

5.5 Gait Selection versus V_F for a Loose Clay Ground

In this sub-section, the study is repeated for a different type of ground, namely a loose clay ground. For this case, the values of the ground parameters yield $K_{xF} = 2.6 \times 10^5 \text{ Nm}^{-1}$, $B_{xF} = 7.7 \times 10^5 \text{ Nsm}^{-1}$, $K_{yF} = 3.4 \times 10^5 \text{ Nm}^{-1}$ and $B_{yF} = 4.7 \times 10^5 \text{ Nsm}^{-1}$.

Figure 8 presents the chart of $\min[E_{av}(V_F)]$. This index points out that the locomotion should be Canter, Amble, Trot and Bound, as the speed increases. The other gaits lead to values of $\min[E_{av}(V_F)]$ higher than these ones, for all range of V_F . In particular, the gaits Walk and Chelonian Walk lead to the higher values of this performance measure.

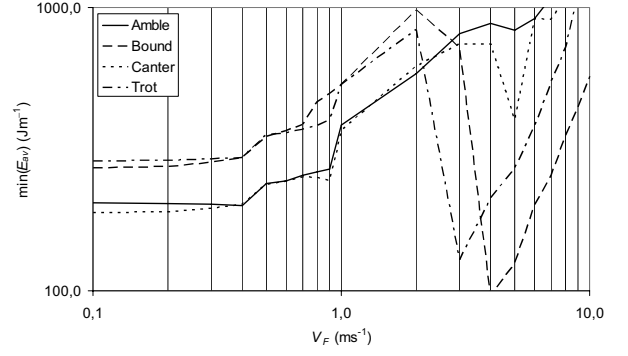


Fig. 8. $\min[E_{av}(V_F)]$ for $F_C = 0.1 \text{ m}$, considering the optimum values of L_S and H_B , and a robot walking on a ground of loose clay.

5.6 Gait Selection versus V_F for a Peat Ground

The study is extended to a very soft ground, consisting of peat, in which the robot feet may become stuck. For this case, the values of the ground parameters are given by $K_{xF} = 4.3 \times 10^4 \text{ Nm}^{-1}$, $B_{xF} = 6.7 \times 10^4 \text{ Nsm}^{-1}$, $K_{yF} = 5.7 \times 10^4 \text{ Nm}^{-1}$ and $B_{yF} = 4.8 \times 10^4 \text{ Nsm}^{-1}$.

The chart of $\min[E_{av}(V_F)]$, for the different gaits, is presented in Figure 9. It is concluded that the most efficient way to perform the locomotion, measured through the index E_{av} , is to adopt the Amble gait for $V_F < 1.0 \text{ ms}^{-1}$, the Rotary Gallop gait for $1.0 \text{ ms}^{-1} < V_F < 2.0 \text{ ms}^{-1}$, the Trot gait for $2.0 \text{ ms}^{-1} < V_F < 4.0 \text{ ms}^{-1}$ and the Bound gait for $V_F > 4.0 \text{ ms}^{-1}$. All the remaining gaits under study lead to values of $\min[E_{av}(V_F)]$ higher than these ones, on all range of V_F .

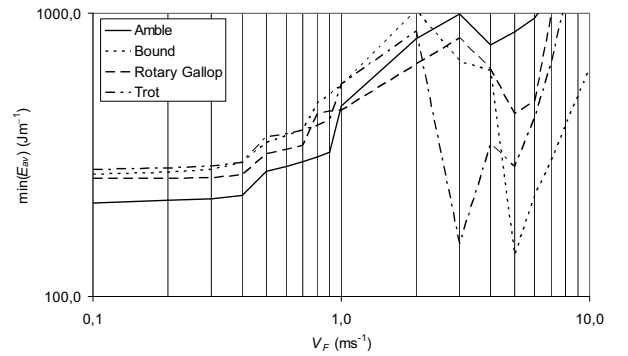


Fig. 9. $\min[E_{av}(V_F)]$ for $F_C = 0.1 \text{ m}$, considering the optimum values of L_S and H_B , and a robot walking on a ground of peat.

5.7 Discussion of the Results

From the above results we can conclude that, from the viewpoint of E_{av} , the robot gait should change with the desired forward body velocity. These results seem to agree with the observations of the living quadruped creatures [12].

In general terms, the values of $\min[E_{av}(V_F)]$ increase with V_F . The increasing is more pronounced for the walking gaits {Walk, Chelonian Walk and Amble}. For the case of the running gaits {Trot, Pace, Canter, Transverse Gallop, Rotary Gallop, Half-Bound and Bound} there is a minimum of this index for $V_F > 0.9 \text{ ms}^{-1}$, being this minimum more pronounced when L_S and H_B are adapted to the locomotion velocity.

Comparing the results of the different experiments we conclude that, as observed in nature, the walking gaits are more adequate for low / moderate velocities, while the running gaits should be adopted for high velocities. In what concerns the Bound gait, all experiments indicate it as the optimum gait at the upper limit of the tested range of velocities.

In conclusion, the locomotion gait and the parameters L_S and H_B should be chosen according with the robot forward velocity (as the speed increases, the value of L_S should be increased and the value of H_B decreased) in order to optimize the energy efficiency and the oscillation of the hips trajectories.

Concerning the minimum values of the performance index \mathcal{E}_{xyH} , although not presented in this article, the experiments reveal that the walking gaits {Walk, Chelonian Walk and Amble} allow the locomotion with lower hip trajectories oscillations, and the asymmetrical running gaits (in particular the Half-Bound and Bound) impose the higher oscillations in the hips trajectories.

6. Conclusion

In this paper we have compared several aspects of periodic quadruped locomotion gaits. By implementing different motion patterns, we estimated how the robot responds to the locomotion parameters step length and body height and to the forward speed.

For analyzing the system performance two quantitative measures were defined based on the system energy consumption and on the hip trajectory errors.

A set of experiments determined the best set of gait and locomotion variables, as a function of the forward velocity V_F , and for different characteristics of the robot intra-body compliance and different types of ground.

The results show that the locomotion parameters should be adapted to the walking velocity in order to optimize the robot performance. As the forward velocity increases, the value of L_S should be increased and the value of H_B decreased. Furthermore, for the case of a quadruped robot, we concluded that the gait should be adapted to V_F .

While our focus has been on a dynamic analysis in periodic gaits, certain aspects of locomotion are not necessarily captured by the proposed measures. Consequently, future work in this area will address the refinement of our models to incorporate more unstructured terrains, namely with distinct characteristics of the ground. Bearing these ideas on mind, we plan to develop this analysis process in just

one phase, simultaneously finding the optimum values of the parameters L_S and H_B and of the gait, versus V_F , through the use of genetic algorithms.

Acknowledgements

The authors would like to thank GECAD – *Grupo de Investigação em Engenharia do Conhecimento e Apoio à Decisão*, of Institute of Engineering of Porto, for their financial support to this work.

References

- [1] I. Poulakakis, J.A. Smith & M. Buehler, Experimentally Validated Bounding Models for the Scout II Quadruped Robot, *Proc. of the 2004 IEEE Int. Conf. on Robotics & Automation*, New Orleans, USA, 2004.
- [2] F. Iida & R. Pfeifer, "Cheap" Rapid Locomotion of a Quadruped Robot: Self-Stabilization of Bounding Gait, *Proc. of the 8th Conf. on Intelligent Autonomous Systems*, Amsterdam, The Netherlands, 2004.
- [3] N. Kohl & P. Stone, Policy Gradient Reinforcement Learning for Fast Quadrupedal Locomotion, *Proc. of the 2004 IEEE Int. Conf. on Robotics & Automation*, New Orleans, USA, 2004.
- [4] L.R. Palmer, D.E. Orin, D.W. Marhefka, J.P. Schmiedeler & K.J. Waldron, Intelligent Control of an Experimental Articulated Leg for a Galloping Machine, *Proc. of the 2003 IEEE Int. Conf. on Robotics & Automation*, Taipei, Taiwan, 2003.
- [5] M. Hardt & O. von Stryk, Towards Optimal Hybrid Control Solutions for Gait Patterns of a Quadruped, *Proc. 3rd Int. Conf. on Climbing and Walking Robots*, Madrid, Spain, 2000.
- [6] M.F. Silva, J.A.T. Machado & A.M. Lopes, Modelling and Simulation of Artificial Locomotion Systems, *ROBOTICA*, 23(5), 2005, 595 – 606.
- [7] URL: <http://www.biology.leeds.ac.uk/teaching/3rdyear/Blgy3120/Jmvr/Loco/Gaits/GAITS.htm> **[2006-08-09]**
- [8] M.F. Silva, J.A.T. Machado, A.M. Lopes & J.K. Tar, Gait Selection for Quadruped and Hexapod Walking Systems, *Proc. of the 2004 IEEE Int. Conf. on Computational Cybernetics*, Vienna, Austria, 2004.
- [9] M.F. Silva, J.A.T. Machado & A.M. Lopes, Energy Efficiency of Quadruped Gaits, *Climbing and Walking Robots*, M. O. Tokhi, G. S. Virk and M. A. Hossain (Eds.), Springer, 2006, 735–742.
- [10] M.F. Silva, J.A.T. Machado & A.M. Lopes, Position / Force Control of a Walking Robot, *Machine Intelligence and Robotic Control*, 5(2), 2003, 33–44.
- [11] M.F. Silva & J.A.T. Machado, Kinematic and Dynamic Performance Analysis of Legged Systems, Accepted for publication in *ROBOTICA*.
- [12] R. McN. Alexander, The Gaits of Bipedal and Quadrupedal Animal, *The Int. Journal of Robotics Research*, 3(2), 1984, 49–59.